

A 3.5~7.5 GHz GaAs HEMT Cryogenic Low-Noise Amplifier Achieving 5 Kelvin Noise Temperature for Qubits Measurement

Yatao Peng[#], Youpeng Zhong^{&*}, Zechen Guo^{&*}, Song Liu^{&*}, Dapeng Yu^{&*}

[#]State Key Lab. of Analog and Mixed-Signal VLSI, IME/ECE of FST, University of Macau, China

[&]Shenzhen International Quantum Academy, China

^{*}Shenzhen Institute for Quantum Science and Engineering, SUSTech, China

Abstract—The measurement of the fast-increasing number of qubits necessitates the use of a large number of specialized cryogenic low-noise amplifiers (LNAs). This work presents a broadband LNA designed with discrete GaAs HEMT components which operate well at ~3.6 K temperature. The dual-frequency optimum noise matching network and output matching elements of the first stage were employed to optimize the equivalent noise temperature (NT) and the input return loss in a wideband. Measurement results at 3.6 K ambient temperature show that the LNA achieved an equivalent NT of <12 K, and a gain of >30 dB in the 3.5 GHz to 7.5 GHz band with a minimum of 5 Kelvin at ~6.5 GHz. The best visibility of ~0.891 is achieved when using the LNA to observe a superconducting transmon qubit without using a JPA.

Keywords—cryogenic low noise amplifier, LNA, GaAs, transmon, quantum computer, impedance matching network.

I. INTRODUCTION

Recent trends in quantum computer development are in the direction of the increased number of qubits [1]. Since the qubits are very fragile and sensitive to any kind of noise, the equivalent noise temperature (NT) requirement of the low noise amplifiers (LNAs) operating at a 4 Kelvin plate in a dilution refrigerator (determines the NT of a receiver) is as low as several Kelvins for fast and high-fidelity superconducting transmon qubits and silicon spin qubit measurement [2], [3]. Using a Josephson parametric amplifier (JPA) with < 1 Kelvin NT as the 1st stage in the qubit readout chain as shown in Fig. 1 alleviates the stringent noise requirements of the LNA for the qubit readout. For one thing, since the reciprocity of the JPA and limited isolation of the circulators, although high isolation can be achieved for multiple junctions which also means larger insertion loss, the noise generated by the sequent amplify stages may be kicked back to the quantum devices thus reduce the coherent time of the qubits. For another thing, the JPAs have very limited power handling capacity (or bad linearity) and narrow bandwidth [4] which complicate the system when a mass of the qubits is ready to be observed. Therefore, such quantum systems with thousands even millions of qubits still necessitate a very large number of cryogenic LNAs with low power consumption, sufficient gain, extremely low equivalent noise temperature (NT), and even high linearity when the frequency-division multiplexing (FDM) readout is used.

Traditionally, indium-phosphide (InP) devices are used to achieve cryogenic LNA. However, due to the increasing number of qubits readout channels, the emphasis on cost, yield, and reliability is increased. This leads to a reconsideration of GaAs to replace the more brittle InP, which is also

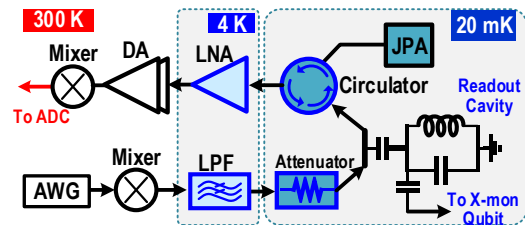


Fig. 1. Typical diagram of a superconducting qubit readout system.

commercially more attractive and allows higher productivity. To implement a cryogenic LNA block, although the GaAs MMIC approach can achieve a more compact footprint, the discrete component approach is more flexible for customized development with shorter design iteration cycles [5]–[7]. This paper reports a cryogenic LNA operating at ~3.6 Kelvin realizing with discrete GaAs HEMT devices aiming for superconducting qubits readout. LNA. The organization of this paper is as follows:

- 1) A wideband input matching network (IMN) with output matching elements as design parameters for achieving wideband optimum noise figure was described. The design considerations for cryogenic operating were discussed.
- 2) The measurement of electronic performances and qubit readout results were presented.

II. DESIGN

The design of the cryogenic LNA was begin with the characterization of the devices at a cryogenic temperature (CT), ~3.6 K Kelvin in our work. The I-V characteristics of the used GaAs HEMTs (CEL3512K2) were tested by sweeping the voltages applied in the drain and gate, which indicates that this device works well at CTs. On the other hand, the cryogenic noise parameters (Γ_{OPT} , R_N , F_{MIN}) used for the cryogenic LNA design were obtained by adjusting the room temperature (RT) data according to the variations concluded in the literature [5]–[8]. Based on these cryogenic device parameters, the topology and the small signal model used for simulation of the cryogenic LNA are illustrated in Fig. 2. The LNA consists of three stages, the first of which is a low-noise stage, the second provides sufficient gain, and the third stage increases gain further while achieving wideband output impedance matching. For the first stage, optimum noise matching (Z_{OPT}) is required which always means the loss of the power matching (Z_{IN}), i.e. a poor S_{11} due to the large mismatch of Z_{OPT} and Z_{IN} of the HEMT device caused by the gate-drain capacitance (C_{gd}) and gate induced

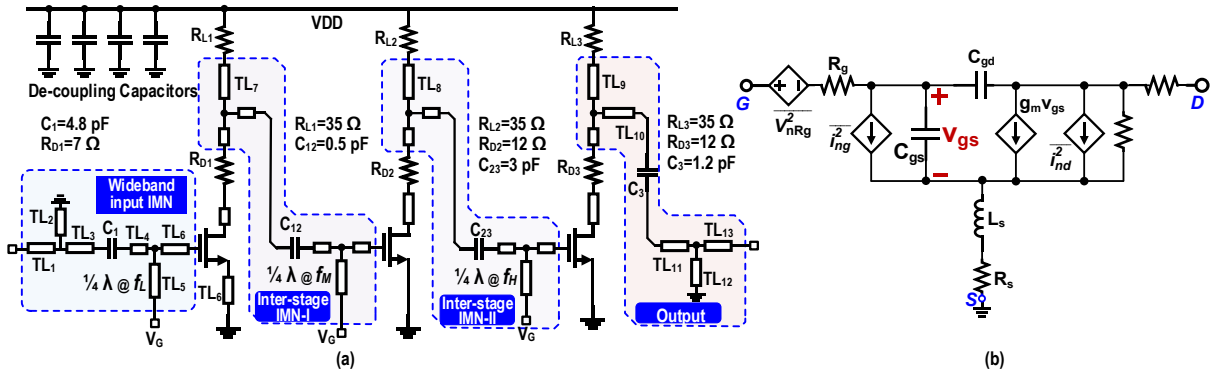


Fig. 2. (a) Schematic of the designed cryogenic LNA. (b) The small signal model.

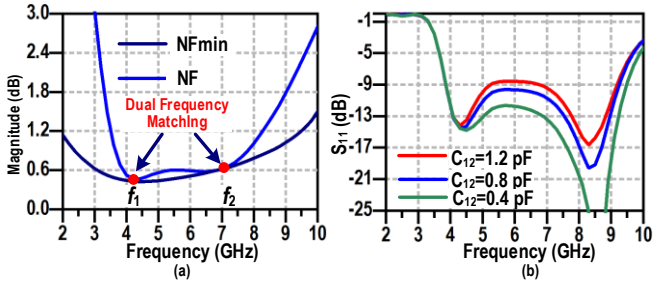


Fig. 3. (a) The dual-frequency matching for optimizing NF. (b) S_{11} versus frequency under different C_{12} .

noise. In our design, the wide-band input impedance matching network (IMN), realized by six transmission line sections (TL₁~TL₆) at the gate and TL₀ at the source of the input transistor M₁, were used to achieve dual-frequency optimum noise impedance [Fig. 3(a)], while the power matching (S_{11}) was optimized by the impedance matching elements at the drain of M₁ (mainly the C₁₂) [Fig. 3(b)]. The inter-stage IMN-I and IMN-II were implicitly implemented by drain and gate biasing elements and the DC-block capacitors. Note that the conjugate matching points of IMN-I and IMN-II were designed at different appropriate frequencies (~4 GHz and 7 GHz) to flatten the gain in the operating band. The resistors R_{D1}~R_{D3} were utilized to reduce the inverse gain (S_{21}) thus stabilizing the LNA with a k -factor greater than 1.1 as high as 20 GHz. The load resistors R_{L1}~R_{L3} around 30 Ω can damp the gain at low frequency to a certain extent (~3 dB) since TL₇~TL₉ transfer R_{L1}~R_{L3} to smaller impedance for low frequency compared with high frequencies, thus further smooth the in-band gain and increase the k -factor. Grounded branch lines (TL₂ and TL₁₂) were purposely introduced into the input and output wideband IMNs to effectively circumvent low-frequency oscillations, which may easily occur at cryogenic temperatures due to the significant increment (~5x) of transconductance (G_M) of the HEMTs at CT compared with RT value.

In order to save power, for a multi-stage amplifier, different circuit stages are designed to have various biasing voltages. Typically, the first stage draws more power for better noise performance, while the other stages are biased at lower drain voltages that compromise linearity, which is often considered less essential when accessing a single qubit per readout chain. These multiple voltages, in practice, require the use of more cryogenic wire resources, which are limited inside a dilution

refrigerator when large-scale qubits need to be handled. Another expense is the necessity for many low-noise DC power suppliers at room temperature to bias the LNA given that no available cryogenic LDO at present, which certainly adds system cost and decreases reliability. Therefore, in our design, we designed the three stages with the same quiescent voltages and currents (2 V supply voltage with 10 mA I_D for RT), where biasing voltages of the 2nd and 3rd stages were aligned with the 1st stage obtaining optimum noise performance, which also facilitates higher linearity. It is critical when FDM readout is applied.

III. IMPLEMENTATION AND MEASUREMENT

The cryogenic LNA was implemented on the Rogers 5880 substrate with the minimum thickness option (0.254 mm) to lower the substrate loss given the metal thermal loss decrease by 10x at 4 K. At cryogenic temperature (~4 Kelvin), the dielectric constant (ϵ_r) decreases less than 6% from its room temperature value (2.55) [8]. Therefore, the IMNs are expected to be able to conduct the impedance transformation properly at CT. The capacitors and the resistors are designed with a 0402 footprint to lower the introduced parasitic capacitance. The PCB dimension is around 27 mm×46 mm and is installed in a bronze box with a non-conductive silicone absorber [Fig. 4(a)], which was pre-verified that functioned well at CT, to avoid the microwave cavity effect and the self-excited oscillation.

The LNA block was first tested at room temperature (RT=297 K) with $V_G=-0.61$ V, $V_{DD}=2$ V, and $I_{DC}=-28$ mA. The scatter parameters, measured by a Rohde & Schwarz vector network analyzer (ZNB 20), are shown in Fig. 5. The gain at RT is 36±2.5 dB in the frequency from ~3 GHz to 7.5 GHz, in which band the S_{11} is <-7 dB and S_{22} is <-10 dB. The RT noise figure is tested by a handheld microwave analyzer Keysight FieldFox N9918A with the noise figure measurement option, and the results are given in Fig. 6. It can be seen the LNA has sub-1 dB NF from ~3.5 GHz to 8 GHz with a minimum NF of 0.75 dB at ~6.4 GHz.

Once the performance at RT was initially verified, more efforts were spent on the characterization of the LNA under CT. As shown in Fig. 4(b) and (c), the LNA modules were installed inside a 4 Kelvin cryostat. The results of S-parameter measurements for two different samples (1# and 2#) at ~3.6 Kelvin are shown in Fig. 7, revealing that the S-parameters

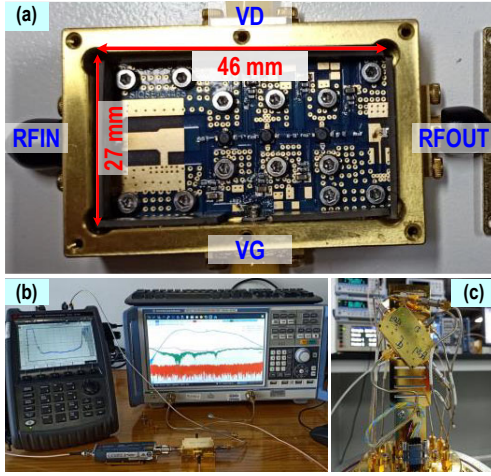


Fig. 4. Photograph of (a) the cryogenic LNA module, (b) the test system configuration, and (c) LNA mounting diagram.

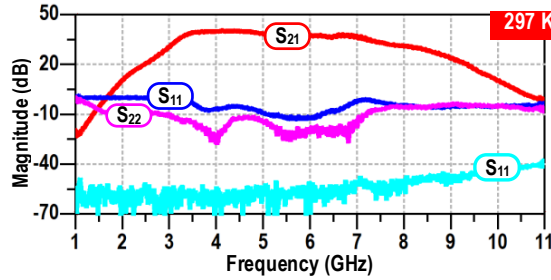


Fig. 5. Measured S-parameters of the LNA at 297 K.

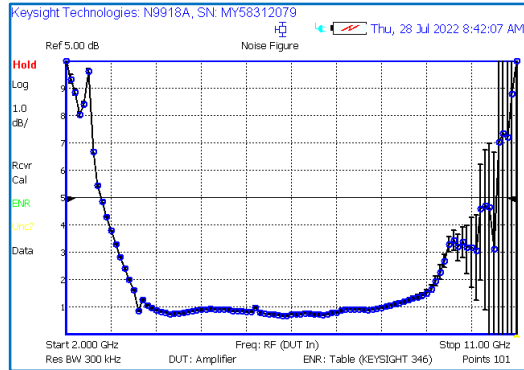


Fig. 6. Measured noise figure of the LNA at 297 K.

remain in good agreement from sample to sample. The LNA consumes a total of 9.5 mA quiescent current under 2 V supply voltage of at CT while obtaining a gain of >30 dB in the 3.5 to 7.5 GHz band. At the same biasing conditions, the noise figure at CT is measured using the cold attenuator setup shown in Fig. 8, where the cold/hot noise sources were provided by the Keysight 346B and a 20 dB coaxial attenuator was used for thermal isolation. Relying on a similar connection, we removed the LNA and measured the insertion loss (L_A) of the attenuator at 3.6 Kelvin and the equivalent NT of the coaxial cables (N-M) since the cables and adapters connected after the LNA have a very small impact on the NT according to Friis Formula for noise. All the obtained results were used to de-embed the influence of the test fixtures (cables, attenuator, and adapters)

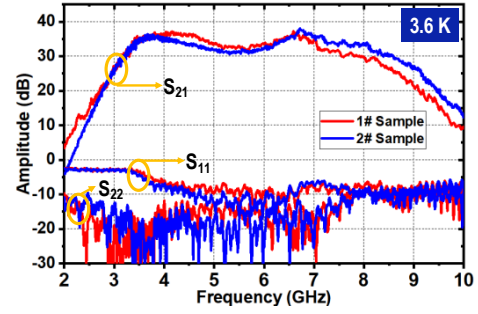


Fig. 7. Measured S-parameters of the LNAs at 3.6 K.

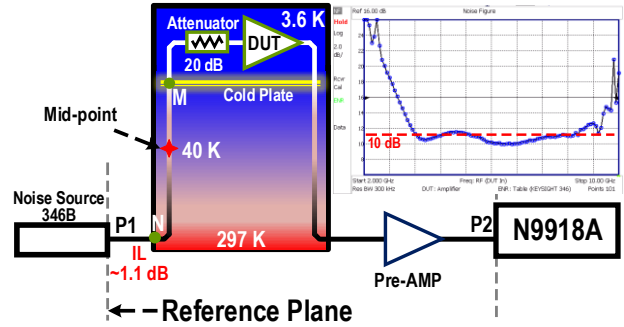


Fig. 8. Diagram showing cold attenuator set-up for measuring the NT of a LNA at CT and the measured noise figure without de-embedding

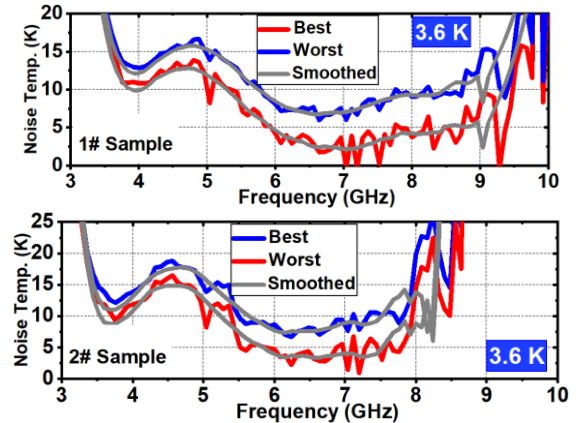


Fig. 9. Measured equivalent NT of the LNAs at 3.6 K

thereby calculating the true noise performance of the LNA modules (1# and 2# sample), which are shown in Fig. 9. As can be seen, the LNA shows ~ 5 K equivalent NT at 6~7 GHz. Note that, the coaxial cable temperature variation pattern from 297 K to 3.6 K is not precisely available (a plausible estimate is ~ 40 K at the midpoint). Furthermore, the equivalent NT of the cryogenic female-to-female adapters used for the de-embedding cannot be well tested. Also, there were impedance mismatches at the output port of the noise source and the input port of the pre-amp. All the above-mentioned factors introduced considerable uncertainty for NT test results of 3.6 K. The OIP3 test results under 297 K and 3.6 K are plotted in Fig. 10, where the offset frequency of the two tones was 20 MHz. It can be seen that the linearity degraded ~ 6 dB at CT, which is the result of an increment of the threshold slope. The k -factors under 3.6 K of the two samples were extracted from their cryogenic S-

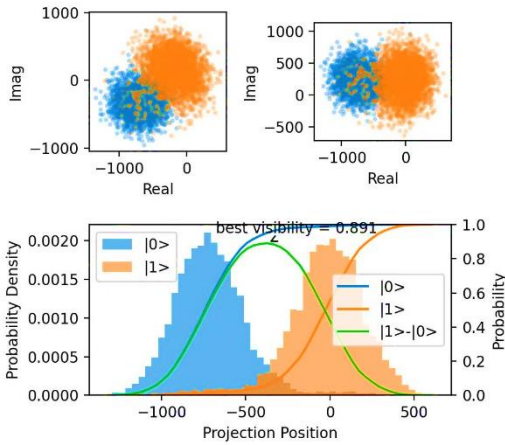


Fig. 11. The measured cryogenic k-factor of the LNAs

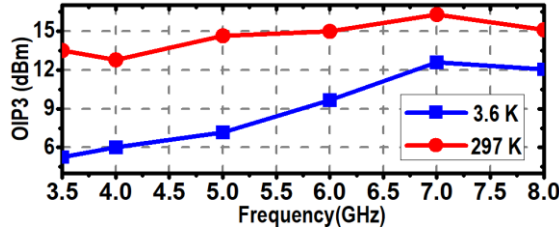


Fig. 10. Measured OIP3 of the LNA with 20 MHz spacing two-tone signals

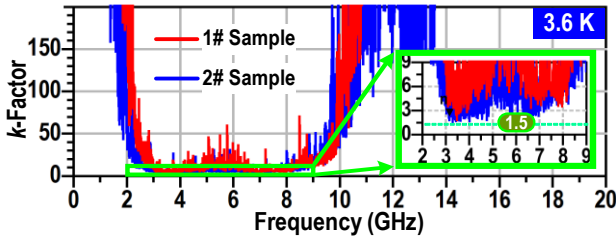


Fig. 12. The achieved I/Q scatter and histogram plots using the designed LNA for superconducting qubit measurement.

parameters and plotted in Fig. 11. The LNAs' k -factors are > 1.5 in the operating band indicating the stability of the LNAs.

In order to validate the LNA, it is linked to a qubit measurement chain with a configuration similar to that shown in Fig. 1. The qubit's readout cavity was designed to operate at 5.5 GHz. In the BlueForce DR, the LNA module was installed on a 4 K plate. One important point is that we do not employ JPA, therefore the noise performance of the entire chain is determined by the NT of the amplifier. The results of the I/Q demodulation [9] for the qubit state are given in Fig. 12, where we got a best visibility of 0.891 for distinguishing states $|0\rangle$ and $|1\rangle$, which is comparable to the figure attained by the cryogenic LNA (0.92 with ~ 3.5 K NT) implemented by InP devices.

IV. CONCLUSION

In this paper, we implemented an LNA that operates at 3.6 K. The LNA has an average gain of 32 dB and a minimum equivalent NT 5 K in the frequency range of 3.5 to 7.5 GHz. This work demonstrates that discrete GaAs devices can be used to achieve cryogenic LNA for transmon qubit readout with demodulation performance comparable to that of the InP LNA.

ACKNOWLEDGMENT

The authors would like to thank Mr. Jad Benserhir and Prof. Edoardo of EPFL for the discussion about the NT test at cryogenic temperatures and Dr. Jian Li of Sustech for building up the cryogenic RF test system. This work was partially supported by the UM start-up research grant of SRG2022-00029-IME.

REFERENCES

- [1] C. Ferner, "Contributions of Quantum Factoring on Quantum Research," *Computer (Long Beach Calif)*, vol. 55, no. 8, pp. 5–7, Aug. 2022, doi: 10.1109/MC.2022.3178307.
- [2] W. T. Wong, M. Hosseini, H. Rucker, and J. C. Bardin, "A 1 mW cryogenic LNA exploiting optimized SiGe HBTs to achieve an average noise temperature of 3.2 K from 4–8 GHz," *IEEE MTT-S International Microwave Symposium Digest*, vol. 2020-August, pp. 181–184, Aug. 2020, doi: 10.1109/IMS30576.2020.9224049.
- [3] Y. Peng, A. Ruffino and E. Charbon, "A Cryogenic Broadband Sub-1-dB NF CMOS Low Noise Amplifier for Quantum Applications," in *IEEE Journal of Solid-State Circuits*, vol. 56, no. 7, pp. 2040–2053, July 2021, doi: 10.1109/JSSC.2021.3073068.
- [4] C. -C. Chiong, D. -J. Huang, C. -C. Chuang, Y. -J. Hwang, M. -T. Chen and H. Wang, "Cryogenic 8–18 GHz MMIC LNA using GaAs PHEMT," 2013 Asia-Pacific Microwave Conference Proceedings (APMC), Seoul, Korea (South), 2013, pp. 261–263, doi: 10.1109/APMC.2013.6695113.
- [5] B. Aja et al., "4–12 GHz and 25–34 GHz cryogenic MHEMT MMIC Low Noise Amplifiers for radio astronomy," 2012 IEEE/MTT-S International Microwave Symposium Digest, Montreal, QC, Canada, 2012, pp. 1–3, doi: 10.1109/MWSYM.2012.6259592.
- [6] S. Qu, X. Wang, C. Zhang and Z. Wang, "6–7 GHz Cryogenic Low-Noise mHEMT-Based Amplifier for Quantum Computing," 2019 Cross Strait Quad-Regional Radio Science and Wireless Technology Conference (CSQRWC), Taiyuan, China, 2019, pp. 1–3, doi: 10.1109/CSQRWC.2019.8799182.
- [7] J. Aumentado, "Superconducting Parametric Amplifiers: The State of the Art in Josephson Parametric Amplifiers," *IEEE Microw Mag*, vol. 21, no. 8, pp. 45–59, Aug. 2020, doi: 10.1109/MMM.2020.2993476.
- [8] S. M. Lardizabal, A. S. Fernandez, and L. P. Dunleavy, "Temperature-dependent modeling of gallium arsenide MESFET's," *IEEE Trans Microw Theory Tech*, vol. 44, no. 3, pp. 357–363, 1996, doi: 10.1109/22.486144.
- [9] J. Liu, W. Shan, T. Kojima, and Q. Yao, "Cryogenic modeling of GaAs-pHEMT and its application in low-power MMIC CLNA design for radio astronomy," *Asia-Pacific Microwave Conference Proceedings, APMC*, vol. 2019-December, pp. 1366–1368, Dec. 2019, doi: 10.1109/APMC46564.2019.9038812.
- [10] A. Caddemi, G. Crupi, and N. Donato, "Microwave characterization and modeling of packaged HEMTs by a direct extraction procedure down to 30 K," *IEEE Trans Instrum Meas*, vol. 55, no. 2, pp. 465–470, Apr. 2006, doi: 10.1109/TIM.2006.864248.
- [11] J. Krupka, J. Breeze, A. Centeno, N. Alford, T. Claussen, and L. Jensen, "Measurements of permittivity, dielectric loss tangent, and resistivity of float-zone silicon at microwave frequencies," *IEEE Trans Microw Theory Tech*, vol. 54, no. 11, pp. 3995–4000, Nov. 2006, doi: 10.1109/TMTT.2006.883655.
- [12] P. Krantz, M. Kjaergaard, F. Yan, T. P. Orlando, S. Gustavsson, and W. D. Oliver, "A quantum engineer's guide to superconducting qubits," *Appl Phys Rev*, vol. 6, no. 2, p. 021318, Jun. 2019, doi: 10.1063/1.5089550.